J. Plasma Physics (2009), *vol.* 75, *part* 3, *pp.* 337–344. © 2008 Cambridge University Press
doi:10.1017/S0022377808007617 Printed in the United Kingdom

Equilibrium properties on the EAST superconducting tokamak

J.P. QIAN[1], B.N. WAN[1], L.L. LAO[2], B. SHEN[1], S.A. SABBAGH[3], J. MENARD[4], Y.W. SUN[1], Y.M. DUAN[1], J.H. LI[1], B.J. XIAO[1], X.Z. GONG[1] and EAST RESEARCH TEAM

[1]Chinese Academy of Science, Institute of Plasma Physics, Hefei, Anhui, China (jpqian@ipp.ac.cn)

[2]General Atomics, San Diego, California 92186-5608, USA

[3]Department of Applied Physics and Applied Mathematics, Columbia University 10027, USA

[4]Princeton Plasma Physics Laboratory, Princeton University, Princeton, NJ 08543, USA

(Received 24 May 2008 and in revised form 4 September 2008, first published online 24 October 2008)

Abstract. The Experimental Advanced Superconducting Tokamak (EAST) has a major radius of $R_0 = 1.75$ m and a midplane halfwidth of 0.5 m. It has been operated with a toroidal magnetic field $B_0 = 2$ T and $I_p \leqslant 500$ kA. The evolution of the plasma equilibrium is analysed between discharges by Equilibrium Fitting Code (EFIT). Limiter, single-null and double-null diverted configurations have been produced. A plasma elongation in the range $1.3 \leqslant \kappa \leqslant 1.9$ and a triangularity in the range $0.1 \leqslant \delta \leqslant 0.55$ have been sustained. The operation space of elongated discharges is also presented based on the EAST database.

1. Introduction

The Experimental Advanced Superconducting Tokamak (EAST) is a non-circular device that is intended to develop a steady-state-capable superconducting tokamak to establish the scientific and technological basis for future reactors [1]. It will address advanced physics issues such as the extension of the present stability and performance boundaries of tokamak operation and develop methods to achieve steady-state operation of tokamak fusion reactors using a non-inductive current drive.

In the first experimental campaign, we have successfully obtained reliable plasma initiation, current ramp up and RZIP plasma control (RZ: R and Z positions, IP: plasma current). One principle goal of the second operational campaign has been to obtain shaped diverted plasma using an optimized plasma control algorithm. Limiter, single-null and double-null diverted configurations have been produced in this campaign [2].

For the EAST device, a primary goal has been to establish reproducible plasma configurations required for future experimentation. A basic and essential

https://doi.org/10.1017/S0022377808007617 Published online by Cambridge University Press

component of the analysis of these shapes is the accurate reconstruction of magnetohydrodynamic (MHD) equilibria based on experimental measurements. The basic techniques used in the EFIT code are described in Sec. 2. Details of the reconstruction for the EAST device are discussed in Sec. 3. The experimental production of the main configurations of EAST, along with several illustrative examples, is discussed in Sec. 4. An overview of the operational space and vertical stability for EAST is discussed in Sec. 5. Finally, a summary is given in Sec. 6.

2. Equilibrium technique

In an axisymmetric toroidal system, the MHD equilibrium Grad–Shafranov equation can be written as

$$\Delta^{*}\psi = -\mu_0 R J_t, \quad J_t = RP'(\psi) + \frac{\mu_0 FF'(\psi)}{4\pi^2 R}. \tag{2.1}$$

Here, R is the cylindrical radial coordinate, J_t is the toroidal current density in the plasma, ψ is the poloidal magnetic flux per radian, $F = 2\pi R B_\phi/\mu_0$ and B_ϕ are the poloidal current function and the toroidal magnetic field. The toroidal plasma current is defined by the two flux functions P' and FF', which are the plasma pressure gradient and poloidal current functions, respectively. In general, the two flux functions are arbitrary with a set of free parameters used to allow the self-consistent solution of the equilibrium constraint and minimization of the difference between measured and computed values in a least-squares fitting. As in [3], a general set of polynomial basis functions is chosen of the form

$$P'(\psi) = \sum \alpha_n y_n(x), \tag{2.2}$$

$$FF'(\psi) = \sum \gamma_n y_n(x), \tag{2.3}$$

where x is the poloidal flux normalized to the poloidal flux between the plasma boundary and the magnetic axis. The values of α_n and γ_n are determined by fitting to the available data. In addition, the specific choice of the constraints of these functions for EAST is discussed in section 3.

3. EAST implementation

The EFIT code has been applied to many tokamaks [3,4], and each implementation has the specific features required. EAST reconstructions typically utilize data from magnetic diagnostics including poloidal field (PF) coil currents, with 37 flux loops, 76 magnetic probes (with the tangential and normal directions together) and a Rogowski coil measuring the total toroidal current in the plasma, and a double vacuum vessel and other structures included. Figure 1 shows the polodial cross-section of the EAST device, illustrating the diagnostics, vacuum vessel, PF coils and typical double-null configuration from the fixed boundary calculation.

Special aspects of the EAST EFIT implementation are primarily due to the large vessel current ratio of the total toroidal current (∼10–20%). The vacuum vessel was divided into 40 segments and a Fourier expansion method was used to decrease the unknowns in the reconstruction [5]. The values computed by the fit, and the resulting current in the vessel, agree with the value measured by the plasma current Rogowski coil within the stated error (3%).

https://doi.org/10.1017/S0022377808007617 Published online by Cambridge University Press

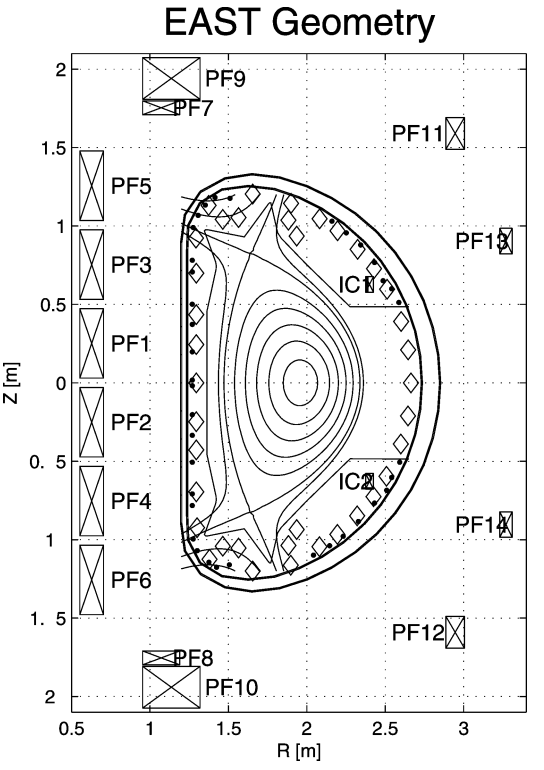


Figure 1. The design of the EAST has an up-down symmetry, with the following parameters: $R = 1.75$ m, $a = 0.5$ m, $B_\phi = 3.5$ T. $I_\mathrm{p} = 1$ MA. Flux loops (closed circles) and magnetic probes (open diamonds) are presented in the figure.

Another consideration for the equilibrium fitting is the choice of constraints for the basis function (P' and FF'). For plasmas with a sufficiently non-circular cross-section ($K > 1.3$) β_p and l_i can be separated from external magnetic measurements alone [6] (Here, poloidal plasma beta $\beta_\mathrm{p} = 2\mu_0 \int_\Omega dV\, P/(B_\mathrm{pa}^2\Omega)$ and internal plasma inductance $l_\mathrm{i} = \int_\Omega dV\, B_\mathrm{p}^2/(B_\mathrm{pa}^2\Omega)$). This indicates that three free parameters can be used to describe three global parameters for the equilibrium, β_p, l_i and I_p. For EAST, a reliable basis function set for P' and FF' is

$$P'(\psi) = \alpha_0 + \alpha_1\psi_n - (\alpha_0 + \alpha_1)\psi_n^2, \tag{3.1}$$

$$FF'(\psi) = \gamma_0 + \gamma_1\psi_n - (\gamma_0 + \gamma_1)\psi_n^2. \tag{3.2}$$

For this model, which has four free parameters, a weak constraint $0.1\alpha_0 + 0.1\alpha_1 = 0$ is imposed. If the number of terms of FF' is set to three to describe more complex profiles, another weak constraint $0.1\gamma_0 + 0.1\gamma_1 + 0.1\gamma_2 = 0$ needs to be imposed [7].

Basis function models of lower order and with different constraints have been tried; the model given above correlated well with the behaviour of $q_0 (\approx 1)$ and the onset of sawteeth on the flat-top of the plasma current. However, it is hard to produce with the model the onset of sawteeth at the plasma current ramp-up due to the larger and more complex eddy current, i.e. more information should be included to fit q_0 during the plasma current ramp-up stage. This is demonstrated

https://doi.org/10.1017/S0022377808007617 Published online by Cambridge University Press

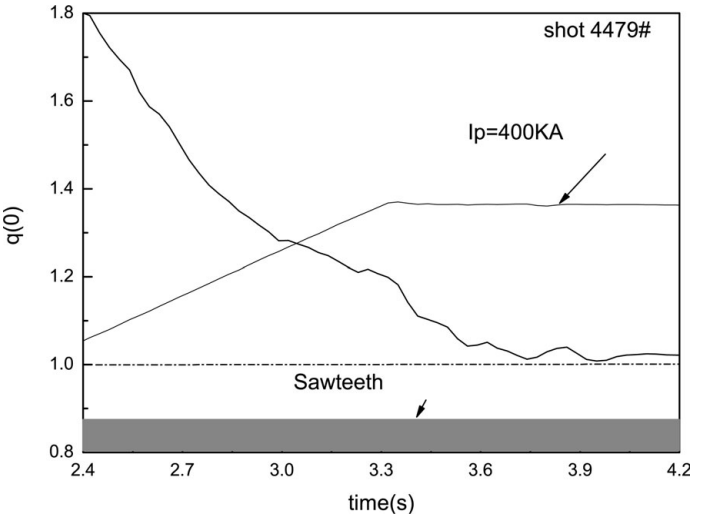


Figure 2. The time of $q_0 = 1$ parallel to the sawteeth at the plasma current flat-top.

in Fig. 2. For all the plasmas with sawteeth examined, sawteeth appeared when $q_0 = 1 \pm 0.05$ at the flat-top of the plasma current.

4. Plasma equilibria

The EAST device has a major radius R_0 of 1.75 m and a midplane halfwidth of 0.5 m. The machine has been operated with ohmic heating in the last two campaigns, with an on-axis vacuum toroidal field of $B_0 = 2$ T and a plasma current of $I_p \leqslant 500$ kA. Pulse lengths have been close to 10 s at $I_p = 200$ kA. The plasma current and the radial and vertical positions are controlled by real-time feedback while the plasma shape is controlled at present by pre-programming currents in PF7 $\sim$ PF10 coils. The vertical stabilization with elongations for diverted plasmas were stably controlled using the (copper) internal control coils.

As discussed in Sec. 3, the equilibrium reconstructions fit the external magnetic measurements well. The evolution of the reconstructed plasma configuration agrees with visible light emission from the plasma. Figure 3 shows a comparison of these results for events that illustrate the plasma boundary in the charged coupled device (CCD). An early, small bore plasma evolution, transition to a double-null diverted plasma is compared with the boundary reconstructions from magnetic diagnostics. The features in the CCD are all consistent with the details of the reconstructed plasma boundary shape. Figure 4 presents the time evolution of the reconstructed magnetic axis and that given by Soft X Ray (SXR) diode arrays with a horizontal view. Note that the latter is determined by the inversion radius when the discharge is sawtoothing. The magnetic axis (vertical position) from the SXR diode (sawtooth) agrees well with the equilibrium analysis.

Figure 5 illustrates the evolution of the plasma parameters for an ohmic elongated plasma with $I_p \approx 300$ kA. The appreciable loop voltage ($\sim$1.8 V) during the plasma current ramp-up stage, the induced currents flowing in the vacuum vessel and the conducting structures about 50 kA ($\sim$16% ratio to the plasma current at the flat-top in this shot) are shown. The plasma stored energy W_{tot} reaches 30 KJ.

https://doi.org/10.1017/S0022377808007617 Published online by Cambridge University Press

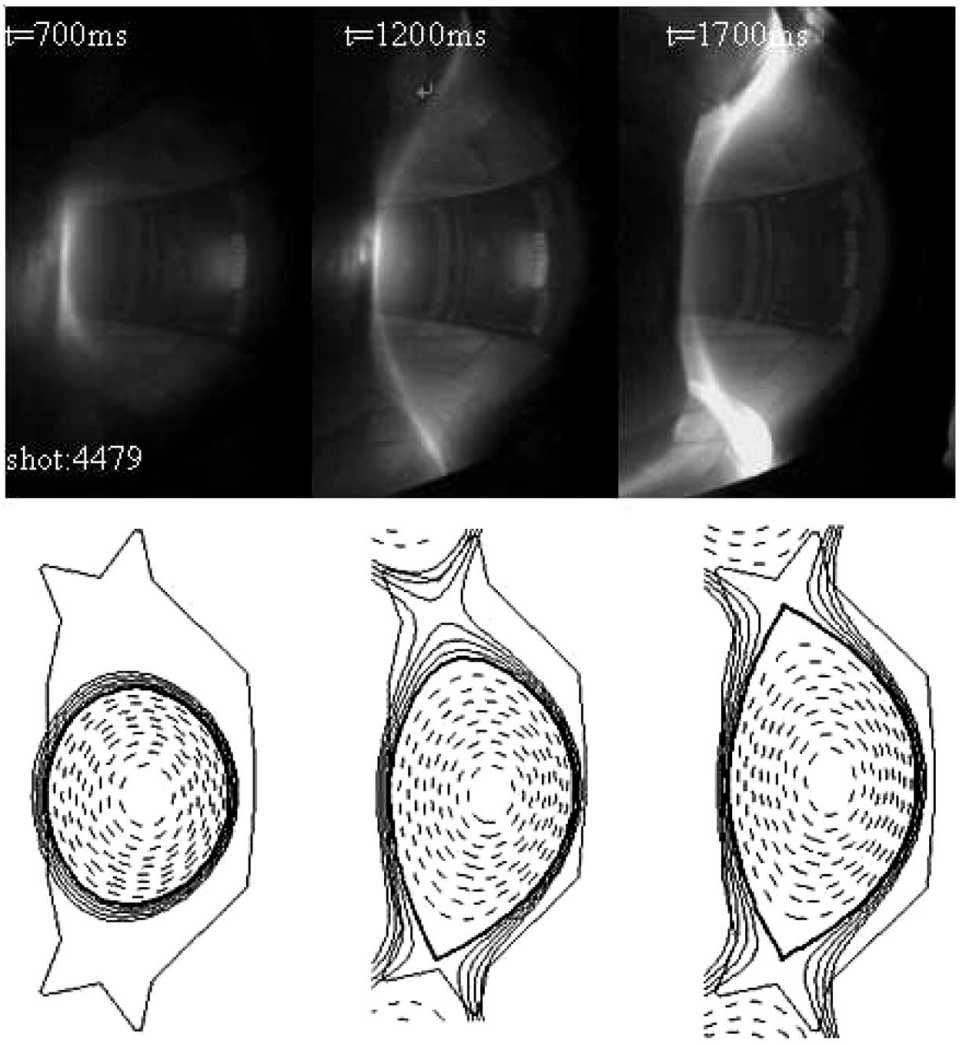


Figure 3. Comparison of the values from the CCD of the plasma boundary and magnetic reconstructions.

The corresponding confinement time τ_{E} is 80 ms (with line-averaged density $\bar{n}_{\mathrm{e}} = 1 \times 10^{19}$ m^{-3}). The ratio $0.85\tau_{\mathrm{E,ITER89P}} \cdot \tau_{\mathrm{E}}/\tau_{\mathrm{E,ITER89P}}$ was approximately 0.8–1.05 at all time slices in this shot.

5. Operational space and vertical stability

A primary goal in the last campaign was to obtain an elongated plasma. Shaped plasmas for EAST were achieved primarily by pre-programming currents in diverted coils. A plasma elongation of $1.3 \leqslant \kappa \leqslant 1.9$ and a triangularity in the range $0.1 \leqslant \delta \leqslant 0.55$ were sustained. The present EAST (κ, δ) database is shown in Fig. 6.

The vertical instability was very serious in EAST with highly shaped plasma configurations. All stable elongated discharges are summarized in Fig. 7, which

https://doi.org/10.1017/S0022377808007617 Published online by Cambridge University Press

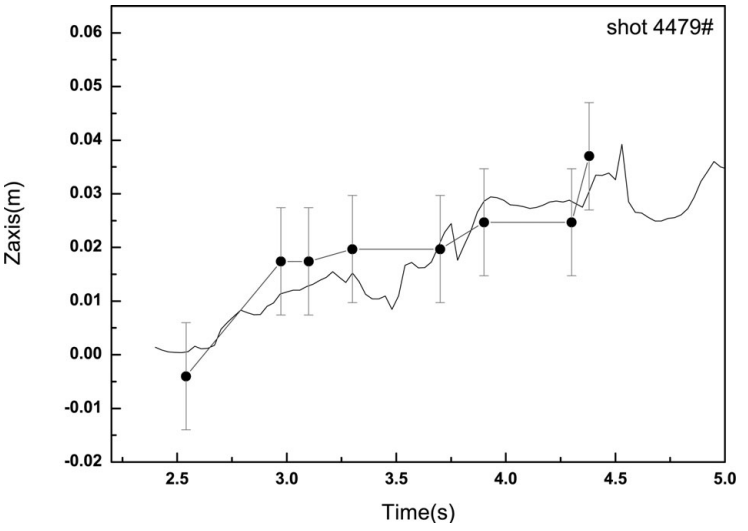


Figure 4. Comparison of the reconstructed Z-axis position (curve) and the axis position with error bars from the SXR diagnostic (points).

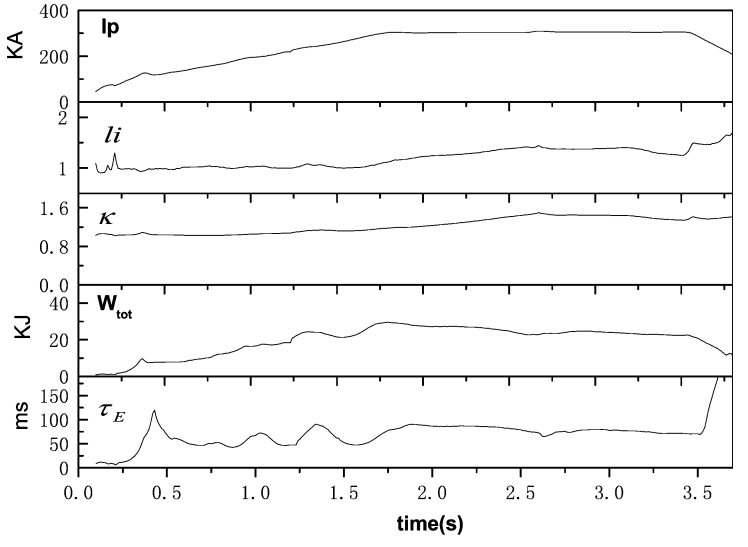


Figure 5. Time evolution of the EFIT reconstructed plasma parameters for an EAST ohmic discharge shot 3975. The interval between reconstructions is 10 ms.

shows the plasma elongation achieved as a function of internal inductance. Each point in the figure represents one EFIT reconstruction from the EAST database. The data has been filtered against rapid vertical motion of plasmas. The guide line in the figure shows an upper bound in the last campaign. As can be seen, plasmas with higher κ and l_i apparently have a destabilizing effect. The dependence of the vertical growth rate on elongation and internal inductance is documented in [8].

https://doi.org/10.1017/S0022377808007617 Published online by Cambridge University Press

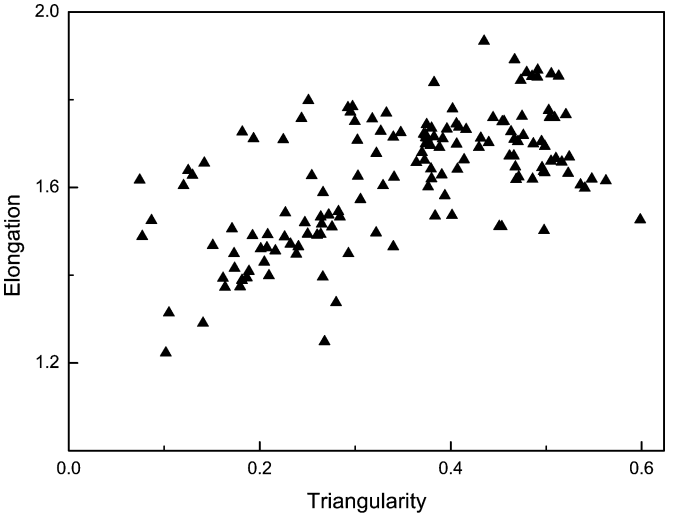


Figure 6. EAST operational space at the plasma current flat-top.

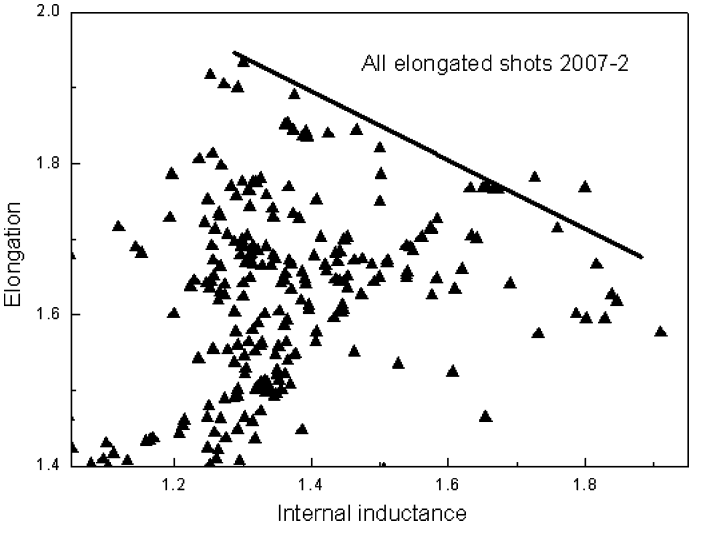


Figure 7. Plasma elongation versus internal inductance for each EFIT reconstruction in the EAST database, filtered against rapid plasma motion. The straight line in the figure is to guide the eye as an upper bound in the last campaign.

6. Summary

EAST equilibria are now reconstructed between discharges using the EFIT algorithm. Details of the plasma boundary shape are all consistent with the features in the CCD. The limiter, single-null and double-null diverted configurations sustained have been produced and reconstructed. The maximum plasma current attained is about 500 kA and pulse lengths have been close to 10 s at $I_p = 200$ kA. The magnetic axis positions from the SXR diode agree with those reconstructed from the EFIT code. The values of q_0 from fitting to the magnetic signals alone can be

https://doi.org/10.1017/S0022377808007617 Published online by Cambridge University Press

compared with the onset time of the sawteeth when plasmas are at the flat-top. The operational space of all elongated discharges presented will be widened after iso-flux/rtefit control in the next campaign.

Acknowledgements

This work was supported by the National Nature Science Foundation of China (No. 10725523) and the Ministry of Science and Technology of the People's Republic of China (No. 2007DFA11290).

References

[1] Yuanxi, W. 2000 *Nucl. Fusion* **40**, 1057.
[2] Baonian, W. et al. 2006 *Proc. 21th IAEA Fusion Energy Conf.*, Chengdu, China.
[3] Lao, L. L., St. John, H. and Stambaugh, R. D. 1985 *Nucl. Fusion* **25**, 1611.
[4] O'Brien, D. P. et al. 1992 *Nucl. Fusion* **32**, 1351.
[5] Qian, J. et al. *J. Plasma Phys.* submitted.
[6] Lao, L. L. et al. 1985 *Nucl. Fusion* **25**, 1421.
[7] Lao, L. L. et al. 2005 *Fusion Sci. Technol.* **48**, 968.
[8] Hofmann, F. 1998 *Nucl. Fusion* **38**, 1767.

https://doi.org/10.1017/S0022377808007617 Published online by Cambridge University Press